

Ion diffusion at charged interfaces
A stochastic dynamics simulation test of the
Smoluchowski-Poisson-Boltzmann approximation

by TORBJÖRN ÅKESSON and BO JÖNSSON

Physical Chemistry 2, Chemical Center, POB 124,
S-221 00 Lund, Sweden

BERTIL HALLE

Physical Chemistry 1, Chemical Center, POB 124,
S-221 00 Lund, Sweden

and DEREK Y. C. CHAN

Department of Mathematics, University of Melbourne,
Parkville, Victoria 3052, Australia

(Received 19 July 1985; accepted 4 November 1985)

We investigate the statistical-mechanical basis and the numerical accuracy of the Smoluchowski-Poisson-Boltzmann (SPB) approximation for describing ion diffusion in non-uniform electrolytes. The many-particle generalized Smoluchowski equation is formally reduced to a hierarchy of coupled n -particle equations. A closure relation, called the Instantaneous Relaxation Approximation (IRA), is used to decouple the equation for the one-particle self-propagator. Introducing also a mean field approximation (MFA), we recover the SPB equation. The accuracy of the IRA and MFA is quantitatively assessed for a model system consisting of two parallel uniformly charged plates with an intervening solution containing point ions in a dielectric medium. This is done by comparing diffusion propagators, survival probabilities and mean first passage times obtained by (1) solving the many-particle generalized Smoluchowski equation by the stochastic dynamics simulation technique (2) numerically solving the one-particle Smoluchowski equation with the exact (simulated) equilibrium potential of mean force, and (3) analytically solving the SPB equation. The IRA is found to be a useful approximation, whereas the MFA can lead to substantial error for systems with strong Coulomb coupling, as in the case of polyvalent counterions. Provided with a realistic potential of mean force, the one-particle Smoluchowski equation thus yields an accurate description of ion diffusion in non-uniform electrolytes.

1. INTRODUCTION

The electric double layer, consisting of an ionic solution in contact with a charged interface, emerges as a central feature of many problems in colloid science, electrochemistry and biophysics. Since the pioneering work of Gouy [1] and Chapman [2], a vast literature has accumulated concerning the derivation,

accuracy and application of the Poisson–Boltzmann (PB) equation and other theories of the equilibrium ion distribution in the double layer. For a recent review, see Carnie and Torrie [3]. Although of considerable importance, the dynamic properties of the double layer have received much less attention [4].

In this paper, we focus on the self-diffusion of the counterions making up the diffuse part of the electric double layer. This problem has been approached in two fundamentally different ways. Historically, the first approach was the association theory [5], which postulates the existence of bound and free counterions with zero mobility and bulk mobility, respectively. This phenomenological approach is still widely used to interpret experimental data. A more realistic picture of the dynamic consequences of the long-range Coulomb interaction is provided by the Smoluchowski approach. Here Smoluchowski's diffusion equation [6]

$$\frac{\partial}{\partial t} f_s(\mathbf{r}; t | \mathbf{r}_0) = D_0 \nabla \cdot [(\nabla - \beta \mathbf{K}) f_s(\mathbf{r}; t | \mathbf{r}_0)] \quad (1)$$

for the space-time evolution of the self-propagator $f_s(\mathbf{r}; t | \mathbf{r}_0)$ is extended by substituting for the external force \mathbf{K} (a uniform gravitational field in Smoluchowski's original application) the equilibrium solvent-averaged mean force acting on a counterion located at \mathbf{r} . When the mean force is evaluated in the Poisson–Boltzmann approximation we shall refer to equation (1) as the Smoluchowski–Poisson–Boltzmann (SPB) equation. The SPB approach, which was pioneered in the double layer context by Lifson and Jackson [7], has proven successful in explaining counterion self-diffusion [8–10] and spin relaxation [11, 12] data from polyelectrolyte solutions.

The aim of this paper is to investigate some of the statistical-mechanical approximations inherent in the SPB equation. Starting from a many-particle generalized Smoluchowski equation, we identify the further approximations that are needed to obtain the SPB equation. These are (1) an assumption of instantaneous response of the surrounding counterions to the motion of the tagged counterion and (2) a neglect of the equilibrium pair correlation among the counterions. (In a uniform electrolyte solution, approximation (1) corresponds to the neglect of the relaxation effect [13].) We then assess the effect of each of these approximations for a model system consisting of two parallel charged plates with an intervening solution containing the counterions, see figure 1. This is accom-

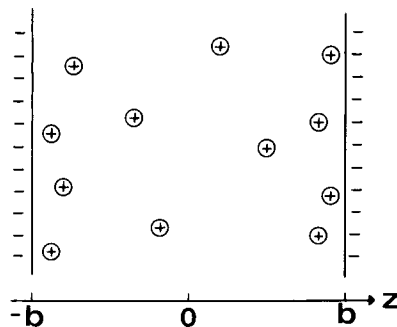


Figure 1. A schematic picture of the model system with the mobile ions, considered as point charges, in between the uniformly charged walls.

plished by solving the many-particle generalized Smoluchowski equation by the Stochastic Dynamics simulation technique and comparing the resulting self-propagator with that obtained (1) by numerically solving the Smoluchowski equation, equation (1), with the exact simulated mean force and (2) by analytically solving the SPB equation. Comparisons are also made of mean first passage times and survival probabilities, formally obtained by integrating the self-propagator over time and/or space.

2. THE GENERALIZED SMOLUCHOWSKI EQUATION

Our point of departure will be the N -particle generalized Smoluchowski equation which governs the time evolution of the probability density $F(\mathbf{r}^N; t | \mathbf{r}_0^N)$ for the configuration of the N counterions

$$\frac{\partial}{\partial t} F(\mathbf{r}^N; t | \mathbf{r}_0^N) = D_0 \sum_{i=1}^N \nabla_i \cdot \left\{ \nabla_i F(\mathbf{r}^N; t | \mathbf{r}_0^N) + \beta \nabla_i \left[u_1(\mathbf{r}_i) + \sum_{j=1}^N u_2(\mathbf{r}_i, \mathbf{r}_j) \right] F(\mathbf{r}^N; t | \mathbf{r}_0^N) \right\}. \quad (2)$$

For definitions of the quantities appearing in equation (2); see Appendix A.

Equation (2) may be derived from the Liouville equation and certain well-defined approximations [14–17]. These are as follows: (1) the relaxation of ionic and solvent momenta and of solvent configuration is fast compared to the time-scale for relevant changes in the ionic configuration, (2) the potential energy of interaction,

$$u_1(\mathbf{r}_i) + \sum_{j=1}^N u_2(\mathbf{r}_i, \mathbf{r}_j), \quad (3)$$

and its derivatives vary negligibly over the ionic momentum correlation length, $D_0(m\beta)^{1/2}$, and (3) the solvent-mediated dynamic coupling between the ions and with the walls may be neglected. Although these approximations do not appear to have been rigorously justified for aqueous electrolytes, simple numerical estimates tend to be reassuring. In this study, however, we shall not be concerned with the accuracy of these approximations. Rather, we shall examine the further approximations that are needed to derive the SPB equation from equation (2).

The first step in our formal derivation of the SPB equation is the reduction of the N -particle generalized Smoluchowski equation, equation (2), to a corresponding equation for the one-particle self-propagator $f_s(\mathbf{r}; t | \mathbf{r}_0)$. As defined in Appendix A, $f_s(\mathbf{r}; t | \mathbf{r}_0) d\mathbf{r}$ is the probability of finding, at time t , the tagged ion to within $d\mathbf{r}$ of \mathbf{r} , given that it was initially at \mathbf{r}_0 . Using the time dependent distribution functions defined in Appendix A, we perform this reduction in Appendix B. The result, equation (B 11), may be expressed in the physically perspicuous form

$$\frac{\partial}{\partial t} f_s(\mathbf{r}; t | \mathbf{r}_0) = D_0 \nabla \cdot \{ [\nabla + \beta \nabla w(\mathbf{r}; t | \mathbf{r}_0)] f_s(\mathbf{r}; t | \mathbf{r}_0) \}, \quad (4)$$

with a time dependent potential of mean force $w(\mathbf{r}; t | \mathbf{r}_0)$ given by

$$\nabla w(\mathbf{r}; t | \mathbf{r}_0) \equiv \nabla u_1(\mathbf{r}) + \int d\mathbf{r}' [\nabla u_2(\mathbf{r}, \mathbf{r}')] g(\mathbf{r}, \mathbf{r}'; t | \mathbf{r}_0) f_d(\mathbf{r}'; t | \mathbf{r}_0). \quad (5)$$

In these equations, \mathbf{r} refers to the position of the tagged particle and \mathbf{r}' to the position of any of the $N - 1$ untagged particles. The self-propagator $f_s(\mathbf{r}; t | \mathbf{r}_0)$ and the distinct propagator $f_d(\mathbf{r}'; t | \mathbf{r}_0)$ are generalizations to finite nonuniform systems of van Hove's space-time correlation functions [18]. The definitions and general properties of these propagators and of the time dependent pair correlation function $g(\mathbf{r}, \mathbf{r}'; t | \mathbf{r}_0)$ can be found in Appendix A.

Taken together, equation (4) and the corresponding equation (B 12) for the distinct propagator constitute the lowest level of a hierarchy of coupled n -particle generalized Smoluchowski equations ($n = 1, 2, \dots, N$), which all can be derived along the lines of Appendix B. In order to obtain the self-propagator $f_s(\mathbf{r}; t | \mathbf{r}_0)$, it is necessary to solve the coupled equations, equations (4) and (B 12), subject to an approximate closure which expresses the pair correlation $g(\mathbf{r}, \mathbf{r}'; t | \mathbf{r}_0)$ in terms of known functions. Such a closure has the effect of decoupling the one-particle level from the two-particle level of the hierarchy. If, in addition, we approximate the distinct propagator in equation (5) by some known function, then also the self and distinct one-particle equations decouple and it suffices to solve equation (4).

The time dependence in the potential of mean force $w(\mathbf{r}; t | \mathbf{r}_0)$, as exhibited in equation (5), reflects the finite time required for the $N - 1$ untagged ions to fill the 'correlation hole' at \mathbf{r}_0 left by the tagged ion. As a consequence, the tagged ion experiences a retarding force which tends to slow down the evolution of the self-propagator. The analogous phenomenon in uniform systems is the so-called relaxation effect [13], which is usually pictured as a dynamic asymmetry in the ion atmosphere around the tagged ion.

The second step in our derivation of the SPB equation is the introduction in equation (5) of the Instantaneous Relaxation Approximation (IRA), defined by

$$g(\mathbf{r}, \mathbf{r}'; t | \mathbf{r}_0) f_d(\mathbf{r}'; t | \mathbf{r}_0) = g_{\text{eq}}(\mathbf{r}, \mathbf{r}') f_{\text{eq}}(\mathbf{r}'), \quad (6)$$

where $g_{\text{eq}}(\mathbf{r}, \mathbf{r}')$ and $f_{\text{eq}}(\mathbf{r}')$ are the usual equilibrium pair correlation and singlet distribution functions.

It is clear from Appendix A that $g(\mathbf{r}, \mathbf{r}'; t | \mathbf{r}_0) f_d(\mathbf{r}'; t | \mathbf{r}_0) d\mathbf{r}'$ is the probability of finding, at time t , any one of the $N - 1$ untagged ions to within $d\mathbf{r}'$ of \mathbf{r}' (irrespective of the configuration of the remaining $N - 2$ untagged ions), given that the tagged ion is simultaneously at \mathbf{r} and with the initial configuration of the untagged ions averaged over the conditional equilibrium probability density with the tagged ion fixed at \mathbf{r}_0 . Consequently, equation (6) is exact in the two limits $t = 0$ and $t \rightarrow \infty$. It would be numerically accurate at all times if the tagged ion were to diffuse much more slowly than the untagged ions. The time taken for the untagged ions to develop an equilibrium correlation with the tagged ion would then be short compared to the time required for significant displacements of the tagged ion.

When equation (6) is inserted into equation (5), we find that the potential of mean force in the IRA is simply the exact equilibrium potential of mean force, $w_{\text{eq}}(\mathbf{r})$, given by

$$\begin{aligned} \nabla w_{\text{eq}}(\mathbf{r}) &= \nabla u_1(\mathbf{r}) + \int d\mathbf{r}' [\nabla u_2(\mathbf{r}, \mathbf{r}')] g_{\text{eq}}(\mathbf{r}, \mathbf{r}') f_{\text{eq}}(\mathbf{r}') \\ &= -\beta^{-1} \nabla \ln f_{\text{eq}}(\mathbf{r}), \end{aligned} \tag{7}$$

where the last equality follows from the lowest member of the equilibrium Bogoliubov–Born–Green–Yvon hierarchy [3]. Consequently, the IRA self-propagator evolves towards the correct equilibrium distribution. (This is expected, since equation (6) is exact in the limit $t \rightarrow \infty$).

The other statistical-mechanical approximation needed in our derivation of the SPB equation is a mean field approximation (MFA), according to which the equilibrium pair correlations are neglected by setting [3, 19]

$$g_{\text{eq}}(\mathbf{r}, \mathbf{r}') = 1 \tag{8}$$

in equation (7). As a consequence, the potential of mean force becomes identical to the mean potential

$$w_{\text{eq}}^{\text{MFA}}(\mathbf{r}) = u_1(\mathbf{r}) + \int d\mathbf{r}' u_2(\mathbf{r}, \mathbf{r}') f_{\text{eq}}^{\text{MFA}}(\mathbf{r}') \tag{9}$$

where $f_{\text{eq}}^{\text{MFA}}(\mathbf{r})$ satisfies the integral equation (7) with $g_{\text{eq}}(\mathbf{r}, \mathbf{r}') = 1$. In the MFA, the tagged ion is thus considered as diffusing in the mean potential resulting from statistical averaging over all the N ions. The consequences of the MFA for equilibrium properties have been studied in detail in references [3], [19] and [28].

3. THE SMOLUCHOWSKI–POISSON–BOLTZMANN EQUATION IN PLANAR GEOMETRY

The model system which we have chosen as testing ground for the SPB equation consists of two parallel uniformly charged plates located at $z = \pm b$ with an intervening solution containing point ions of charge Ze imbedded in a homogeneous dielectric of relative permittivity ϵ_r (see figure 1). The charge of the point ions is opposite in sign to that of the plates, so that the system as a whole is electroneutral. In a system such as this, which contains only counterions, it is possible to set the ionic radius to zero. The effects of the two statistical-mechanical approximations (IRA and MFA) in the SPB equation can thus be investigated without interference from finite ion size effects, i.e. all correlations have a purely electrostatic origin. An additional advantage of the absence of coions is the existence of an analytic solution to the SPB equation for this system [20].

Each plate carries a fixed uniform surface charge density σ . The permittivity is taken to be the same on either side of the plate, so that dielectric image forces do not occur. The singlet and pair potentials are then

$$u_1(z) = \text{constant}; \quad -b < z < b, \quad (10)$$

$$u_2(\mathbf{r}, \mathbf{r}') = \frac{(Ze)^2}{4\pi\epsilon_0\epsilon_r|\mathbf{r} - \mathbf{r}'|}. \quad (11)$$

The mean electrostatic potential

$$\psi(z) \equiv (Ze)^{-1} \int d\mathbf{r}' u_2(\mathbf{r}, \mathbf{r}') f_{\text{eq}}(\mathbf{r}') \quad (12)$$

is approximated by the solution [21, 22] of the Poisson–Boltzmann equation subject to the appropriate boundary conditions

$$\psi(z) - \psi(0) = \frac{2k_B T}{Ze} \ln \cos(\kappa z). \quad (13)$$

The reciprocal Debye length, κ , is obtained by solving the transcendental equation

$$\kappa b \tan(\kappa b) = \frac{|Ze\sigma|b}{2\epsilon_0\epsilon_r k_B T} \quad (14)$$

on the interval $0 \leq \kappa b \leq \pi/2$.

In the IRA equation (4) reads

$$\frac{\partial}{\partial t} f_s(\mathbf{r}; t | \mathbf{r}_0) = D_0 \nabla \cdot \{[\nabla + \beta \nabla w_{\text{eq}}(\mathbf{r})] f_s(\mathbf{r}; t | \mathbf{r}_0)\}. \quad (15)$$

Now from the symmetry of our model system, it is clear that a one-point function such as $w_{\text{eq}}(\mathbf{r})$ can depend only on the z coordinate. The operator on the right-hand side of equation (15) can therefore be split into one part which involves only the cylindrical coordinates ρ and φ and another part which involves only the z coordinate. As a consequence, the diffusion parallel to the plates (the lateral diffusion) is statistically independent from the diffusion perpendicular to the plates (the transverse diffusion). (This is not true when time dependent pair correlations are taken into account.) In the IRA, therefore, equation (15) may be decomposed into two separate diffusion equations; one describing the evolution of the lateral self-propagator

$$\frac{\partial}{\partial t} f_s(\rho; t | \rho_0) = \frac{D_0}{\rho} \frac{\partial}{\partial \rho} \left[\rho \frac{\partial}{\partial \rho} f_s(\rho; t | \rho_0) \right], \quad (16)$$

where ρ is the perpendicular distance (parallel to the plates) from the z -axis, and the other describing the evolution of the transverse self-propagator

$$\frac{\partial}{\partial t} f_s(z; t | z_0) = D_0 \frac{\partial}{\partial z} \left\{ \left[\frac{\partial}{\partial z} + \beta w'_{\text{eq}}(z) \right] f_s(z; t | z_0) \right\}, \quad (17)$$

where the prime signifies differentiation with respect to z .

Since the system is laterally unbounded, the solution to equation (16) is simply the Green's function for two-dimensional free diffusion

$$f_s(\rho; t | \rho_0) = (4\pi D_0 t)^{-1} \exp \left[-\frac{(\rho - \rho_0)^2}{4D_0 t} \right]. \tag{18}$$

If, in equation (17), we also invoke the MFA, with $w_{eq}(z)$ replaced by $Zel\psi(z)$ from equation (13), we arrive at the SPB equation for our model system

$$\frac{\partial}{\partial t} f_s(z; t | z_0) = D_0 \frac{\partial}{\partial z} \left\{ \left[\frac{\partial}{\partial z} - 2\kappa \tan(\kappa z) \right] f_s(z; t | z_0) \right\}. \tag{19}$$

In Appendix C we show that the solution to equation (19), with impenetrable boundaries at $z = \pm b$ and with a delta-function initial condition, is

$$\begin{aligned} f_s(z; t | z_0) &= \frac{\kappa}{2} \cot(\kappa b) \sec^2(\kappa z) + \kappa^2 b \frac{\cos(\kappa z_0)}{\cos(\kappa z)} \\ &\times \sum_{n=1}^{\infty} [\delta_{n, \text{odd}} u_n(\kappa z_0) u_n(\kappa z) + (1 - \delta_{n, \text{odd}}) v_n(\kappa z_0) v_n(\kappa z)] \\ &\times \frac{\exp \{ -[(n\pi/2)^2 - (\kappa b)^2](D_0 t/b^2) \}}{[(n\pi/2)^2 - (\kappa b)^2]} \end{aligned} \tag{20}$$

where $\delta_{n, \text{odd}} = 1$ (0) if n is odd (even). Furthermore

$$u_n(\kappa z) \equiv \tan(\kappa z) \cos\left(\frac{n\pi z}{2b}\right) - \frac{n\pi}{2\kappa b} \sin\left(\frac{n\pi z}{2b}\right), \tag{21 a}$$

$$v_n(\kappa z) \equiv \tan(\kappa z) \sin\left(\frac{n\pi z}{2b}\right) + \frac{n\pi}{2\kappa b} \cos\left(\frac{n\pi z}{2b}\right). \tag{21 b}$$

Since $\kappa b < \pi/2$, the exponentials in equation (20) decay with time and in the limit $t \rightarrow \infty$ only the first term, corresponding to the equilibrium distribution $f_{eq}(z)$, remains. In the limit $\kappa b = 0$, equation (20) reduces to the well-known [23] propagator for one-dimensional free diffusion between reflecting boundaries.

4. STOCHASTIC DYNAMICS SIMULATION

The starting point for the Stochastic Dynamics simulations is the extended Langevin equation for the ionic momenta $\mathbf{p}_i(t)$

$$\frac{d}{dt} \mathbf{p}_i(t) = -\zeta \mathbf{p}_i(t) + \mathbf{R}_i(t) + \mathbf{K}_i(\mathbf{r}^N; t). \tag{22}$$

The effects of the solvent are contained in the dissipation coefficient ζ , in the random force $\mathbf{R}_i(t)$ and in the dielectric screening of the ionic interactions. The time dependence of the ionic force $\mathbf{K}_i(\mathbf{r}^N; t)$ is only implicit through the coordinates \mathbf{r}^N and it is evaluated from the potential model in equations (10) and (11)

$$\mathbf{K}_i(\mathbf{r}^N; t) = -\nabla V_i(\mathbf{r}^N) = -\nabla_i \sum_{j=1}^N u_2(\mathbf{r}_i, \mathbf{r}_j). \tag{23}$$

Equation (22) can be formally integrated to obtain

$$\mathbf{r}(t) - \mathbf{r}_0 = (m\xi)^{-1}(\mathbf{p}_0 - \mathbf{p}(t)) + (m\xi)^{-1} \int_0^t dt' [\mathbf{R}(t') + \mathbf{K}(\mathbf{r}^N, t')], \quad (24)$$

where the index i has been dropped. This is still an equation of motion in phase space. However, for a time t , which is long compared to the momentum correlation time ξ^{-1} , we can neglect the first term on the right-hand side of equation (24) and obtain [24]

$$\mathbf{r}(t) - \mathbf{r}_0 = (m\xi)^{-1} \int_0^t dt' [\mathbf{R}(t') + \mathbf{K}(\mathbf{r}^N; t')]. \quad (25)$$

Equation (25) is a stochastic differential equation, which has a solution in the form of a probability density function $W(\mathbf{r}^N; t | \mathbf{r}_0^N)$. In fact it represents N equations coupled through the force $\mathbf{K}(\mathbf{r}^N; t)$. If we restrict ourselves to short times, but still large compared to ξ^{-1} , then $\mathbf{K}(\mathbf{r}^N; t)$ is approximately constant and the N equations decouple to give

$$\mathbf{r}(t) - \mathbf{r}_0 - \mathbf{K}(\mathbf{r}^N; 0)t/m\xi = (m\xi)^{-1} \int_0^t dt' \mathbf{R}(t'). \quad (26)$$

Applying Chandrasekhar's lemma [25] to equation (26) leads to the desired probability density function

$$W(\mathbf{r}; t | \mathbf{r}_0) = (4\pi D_0 t)^{-3/2} \exp[-|\mathbf{r}(t) - \mathbf{r}_0 - \mathbf{K}t/m\xi|^2/4D_0 t] \quad (27)$$

with $D_0 = kT/m\xi$ and $\mathbf{K} = \mathbf{K}(\mathbf{r}^N; 0)$. (The same symbol, e.g. F or W , will be used to denote different functions, identified by their arguments.)

We will now show that W is also a solution to the generalized Smoluchowski equation, equation (2). Let us, in analogy with what we did in order to arrive at equation (26), replace the potential term in equation (2) with a constant \mathbf{K} as is legitimate for short times. Equation (2) then factorizes and we have

$$\frac{\partial}{\partial t} F(\mathbf{r}; t | \mathbf{r}_0) = D_0 \nabla \cdot \{(\nabla - \beta\mathbf{K})F(\mathbf{r}; t | \mathbf{r}_0)\} \quad (28)$$

with

$$F(\mathbf{r}^N; t | \mathbf{r}_0^N) = \prod_{i=1}^N F(\mathbf{r}_i; t | \mathbf{r}_{0i}). \quad (29)$$

It is simple to show that equation (27) is a solution to the Smoluchowski equation. Thus the two routes, equations (2) and (25), are identical ($W \equiv F$) and which way to proceed is purely based on numerical considerations. It seems, however, that the stochastic approach is conceptually simpler and more suitable for numerical computations.

The right-hand side of equation (26) can be interpreted as a random displacement due to collisions with the solvent molecules and we can rewrite equation (26) as

$$\mathbf{r}(t + \Delta t) - \mathbf{r}(t) = \Delta\mathbf{r}(t, \Delta t) = \Delta\mathbf{r}_G(\Delta t) + \mathbf{K}(\mathbf{r}^N; t) \Delta t/m\xi. \quad (30)$$

The random displacement $\Delta \mathbf{r}_G$ has, in the limit of infinite dilution, a gaussian distribution with the first and second moments equal to

$$\langle \Delta \mathbf{r}_G \rangle = 0 \quad (31 a)$$

$$\langle |\Delta \mathbf{r}_G|^2 \rangle = 6D_0 \Delta t. \quad (31 b)$$

We now assume that $\Delta \mathbf{r}_G$ has the same statistical properties at finite concentrations as in an infinitely dilute system, which is consistent with the neglect of the inertial term in equation (24), see also [24]. This means that neither the friction coefficient nor the random force distribution are affected by the extra force $\mathbf{K}(\mathbf{r}^N; t)$. It is then straightforward to solve equation (30) with a time step Δt small enough so that $\mathbf{K}(\mathbf{r}^N; t + \Delta t) \cong \mathbf{K}(\mathbf{r}^N; t)$, but still $\Delta t \gg \xi^{-1}$. The latter requirement has a formal character, since it is related to the mass of the Brownian particle, which is without significance in the diffusion limit. Simulations with time steps of 0.1 and 0.2 ps were within the statistical fluctuations identical and we used the larger value in all simulations presented here. Periodic boundary conditions were applied in the two directions parallel to the charged walls. To guarantee that the flux across the walls is zero (perfect reflection), an ion was allowed to move perpendicularly only if its new position was confined between the walls. This condition leads to the correct equilibrium distribution, as can be verified from the principle of detailed balance.

The electric force acting on an ion was evaluated using the minimum image convention, that is, it was allowed to interact with all ions within a parallelepiped centred on itself. Due to the long range character of the electrostatic force and the limited number of particles explicitly treated (usually 50 counterions), one has to include a correction from the charges outside the simulation box. This can in principle be done self-consistently, that is the originally unknown distribution is approximated by the distribution obtained from an initial simulation. A second simulation will then give an improved distribution, which in turn can be used to approximate the exact one and so on. This approach has some drawbacks: it is for example not obvious that it will converge and it is rather time-consuming. In the present simulations we have approximated the distribution outside the box with the corresponding Poisson-Boltzmann distribution. This approach has been extensively tested in [19], where also a more detailed account is given.

5. CALCULATIONS

In this section we present a quantitative assessment of the accuracy of the SPB approximation in describing counterion diffusion in the model system of figure 1. The effects of the two statistical-mechanical approximations, instantaneous response (IRA) and neglect of equilibrium spatial correlation (MFA), inherent in the SPB propagator, will be examined separately. This can be done by comparing (1) the exact (within the model) SD propagator, obtained from stochastic dynamics simulations as described in §4, (2) the IRA propagator, obtained by numerically solving equation (17) with the exact (simulated) mean force, as described in Appendix D, and (3) the analytic SPB propagator, as given in §3, which involves both the IRA and the MFA. The simulations, as well as other calculations, were done with the following parameter values: $T = 293$ K, $\epsilon_r = 80.36$, $b = 10.5$ Å (except figure 9), $D_0 = 2 \times 10^{-9}$ m² s⁻¹ and $|\sigma| = 0.224$ C m⁻²

(corresponding to one elementary charge per 71.4 \AA^2). The counterion valency was $Z = 1$ or 2 as indicated, corresponding to $\kappa b = 1.3655$ and $\kappa b = 1.4599$, respectively.

The self-propagator $f_s(\rho, \varphi, z; t | \rho_0, \varphi_0, z_0)$ obtained from the simulation may be regarded as the solution to equation (4). Because of the translational symmetry of the model system, this propagator can depend only on the lateral displacement $\Delta\rho = [(x - x_0)^2 + (y - y_0)^2]^{1/2}$, and on the transverse coordinates z and z_0 . In general the transverse and lateral diffusion processes are coupled but one may define a purely transverse propagator by averaging over the lateral displacement. For our model system, then,

$$f_s(z; t | z_0) = \int_0^\infty d(\Delta\rho) f_s(\Delta\rho, z; t | z_0). \quad (32)$$

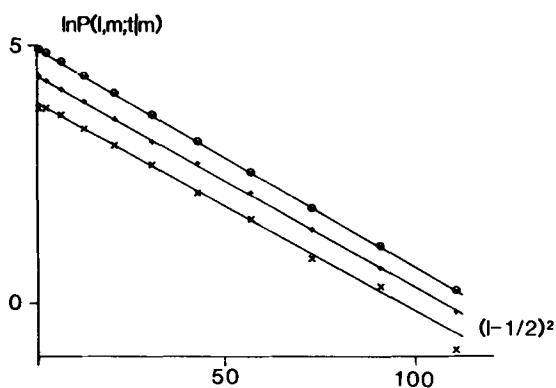
All propagators will be presented in discretized form. Thus $f_s(z; t | z_0)$ is replaced by $P(k; t | k_0)$, which gives the probability of finding the tagged ion in the k th z -interval at time t , given that it was located in k_0 initially. With an interlamellar spacing of 21 \AA and an interval width of 1 \AA , k runs from 1 to 21 ($k = 1$ and 21 being adjacent to the charged walls). The transverse IRA propagator was obtained by first solving equation (17) with a grid spacing of 0.1 \AA and then converting the resulting propagator to the coarser 1 \AA grid used in the figures. The discretization error was found to be negligible. The discretization of the transverse SPB propagator was performed analytically as described in Appendix C.

The lateral diffusion is characterized by the discretized propagator $P(l, m; t | m_0)$, which gives the probability that the tagged ion at time t has suffered a lateral displacement of l radial units, while its initial and final transverse coordinates were in the intervals m_0 and m , respectively. The radial interval width is taken to be 1 \AA ($l = 1, 2, \dots$), while the z -interval is 3.5 \AA so that m runs from 1 to 6 ($m = 1$) and 6 being adjacent to the charged walls).

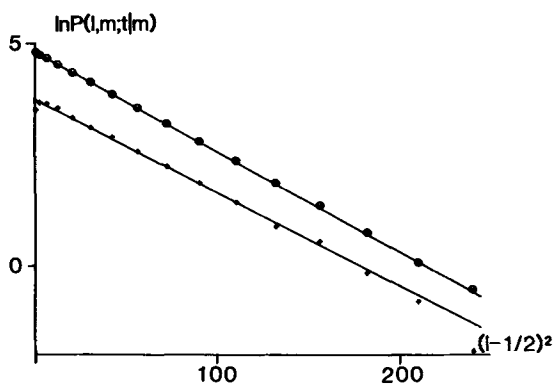
5.1. Lateral propagators

As noted in §3, the IRA and SPB lateral propagators are both independent of the transverse coordinate and given by the free-diffusion Green's function, equation (18). This is a consequence of the symmetry of the model system, which ensures that the (exact) mean force has no lateral component. However, the evolution of the simulated lateral propagator is expected to deviate from equation (18) due to the dynamic correlations associated with the time-dependent mean force in equation (4).

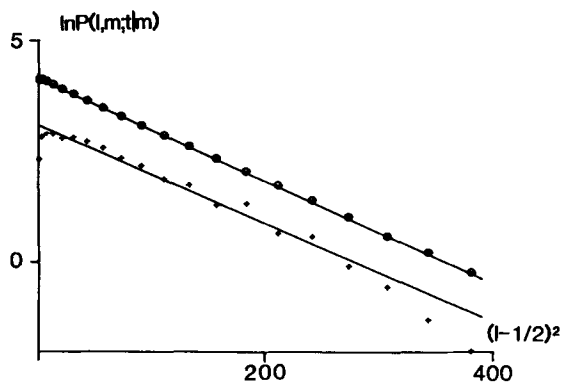
Figure 2 shows the simulated propagator $P(l, m; t | m)$ for monovalent counterions as a function of the square of the lateral displacement. Firstly, we note the almost perfect Gaussian behaviour; the propagators are well described by equation (18) but with an effective diffusion coefficient which is lower than D_0 by up to 15 per cent. This retardation is analogous to the well-known relaxation effect in uniform systems. The second point to note about figure 2 is that the effective diffusion coefficient is time-dependent, i.e. a finite time, of the order 100 ps, is required for the dynamic correlations to be fully manifested. This time



(a)



(b)



(c)

Figure 2. The logarithm of the simulated lateral propagator $P(l, m; t | m)$ for monovalent counterions as a function of $(l - \frac{1}{2})^2$. The straight lines drawn correspond to the logarithm of the Green's function, equation (18), with different values of the diffusion coefficient, D (given below in units of $10^{-9} \text{ m}^2 \text{ s}^{-1}$). To separate the graphs a constant c has been added. (a) $t = 32$ ps: \odot , $m = 1$, $c = \frac{1}{2}$, $D = 1.84$; $+$, $m = 2$, $c = 0$, $D = 1.91$; \times , $m = 3$, $c = -\frac{1}{2}$, $D = 1.94$. (b) $t = 64$ ps: \odot , $m = 1$, $c = 1$, $D = 1.74$; $+$, average for $m = 2$ and $m = 3$, $c = 0$, $D = 1.87$. (c) $t = 128$ ps, $D = 1.70$ and 1.77 respectively. Otherwise as in (b).

may be thought of as a relaxation time for the ionic atmosphere; it should be closely related to the time taken for an ion to diffuse a distance equal to the radius of its 'correlation hole'. Since the counterions accumulate near the walls, this correlation length should be about 6–8 Å (the charge density on each wall corresponds to one elementary charge per $(8.4 \text{ Å})^2$). With a diffusion coefficient of $2 \times 10^{-9} \text{ m}^2 \text{ s}^{-1}$, this yields a relaxation time of about 100–150 ps, in reasonable agreement with the simulations.

In analogy with uniform electrolyte solutions, where the relaxation effect increases with concentration, one expects the lateral diffusion to be maximally retarded near the charged walls where the local counterion concentration is highest. This expectation is borne out by the simulation data in figure 2. From the slopes we thus estimate a diffusivity reduction of *ca* 15 per cent within 3.5 Å of the charged walls (where a counterion resides about 75 per cent of the time), compared to *ca* 8 per cent in the remainder of the system. In view of the large concentration difference between these regions, the observed *z*-dependence in the lateral diffusion may seem surprisingly weak. However, since the inter-lamellar separation is of the same order of magnitude as the correlation length, also counterions midway between the walls are dynamically correlated with those residing near the walls.

5.2. Transverse propagators

In the case of the transverse counterion diffusion, all three calculated propagators (the exact SD propagator and the approximate IRA and SPB propagators) will, in general, be different. Any deviation between the SD and IRA propagators can be traced to dynamic correlations, as in the case of lateral diffusion, whereas a difference between the IRA and SPB propagators reflects static correlations via the equilibrium mean force in equation (17). The discretized transverse propagator, $P(k; t|k_0)$, presented in this subsection refers to reflecting boundary conditions at the charged walls. This propagator evolves towards the equilibrium distribution. In the limit $t \rightarrow \infty$, the SD and IRA propagators should thus coincide, whereas the SPB propagator should exhibit the known [19] deficiencies of the PB approximation for this system, *viz.* a too high counterion concentration in the midplane ($z = 0$) region.

Figures 3–5 illustrate the transverse self-diffusion of monovalent counterions; in figures 3 and 4 we have plotted discretized propagators $P(k; t|k_0)$ as functions of k at fixed time, whereas in figure 5 we plot $P(k; t|k_0)$ as a function of time for given k and k_0 . It is seen that the SD, IRA and SPB propagators agree remarkably well for monovalent ions. Where deviations do occur, they are due mainly to static correlations. This is most clearly seen in the *z*-interval adjacent to the charged wall ($k = 1$) and at long times.

Since the IRA is exact in the two limits $t = 0$ and $t \rightarrow \infty$ (cf. §2), we can expect to see effects of dynamic correlations only at intermediate times. Except for the small differences between the SD and IRA propagators in figures 4 (*b*) and 5 (*b*), there is no indication in figures 3–5 of significant dynamic correlations. In figure 5 (*a*) the SD and IRA $P(1; t|1)$ propagators are seen to coincide at all times. This may be understood on the basis that, at long and intermediate times, dynamic correlations retard to roughly equal extent the counterion fluxes away from and towards the charged wall. On the other hand, at short times, the ion has

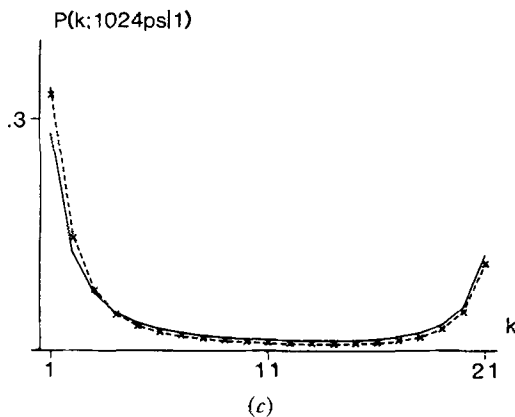
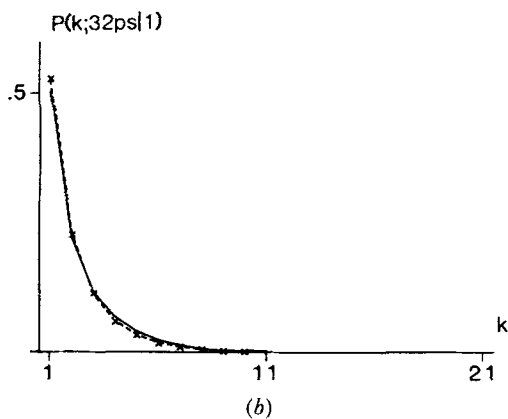
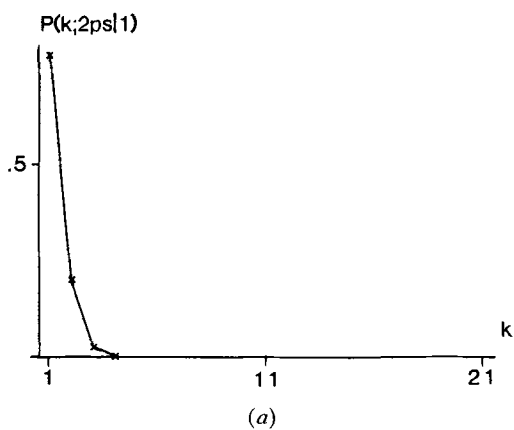


Figure 3. The transverse propagator $P(k; t|1)$ for monovalent counterions as a function of k at three different times: (a) $t = 2$ ps, (b) $t = 32$ ps, and (c) $t = 1024$ ps. Symbols: SD (\times), IRA (----), SPB (—). The standard deviations are about 1 per cent (SD) and 0.2 per cent (IRA).

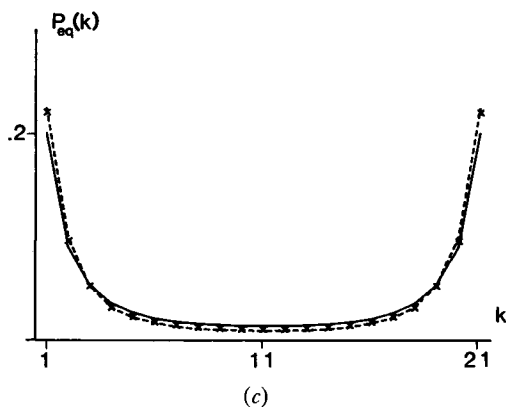
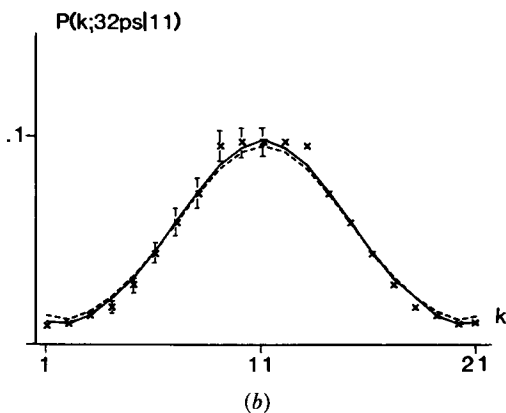
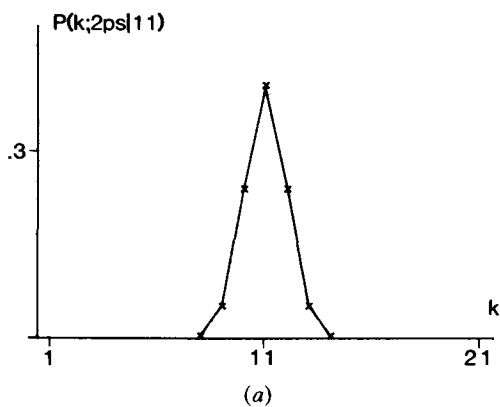


Figure 4. The transverse propagator $P(k; t|11)$ for monovalent counterions as a function of k at two different times: (a) $t = 2$ ps, and (b) $t = 32$ ps. Figure c shows the equilibrium distribution $P_{eq}(k)$. Symbols as in figure 3. The bars show one standard deviation (68.3 per cent confidence limit) for the simulated values.

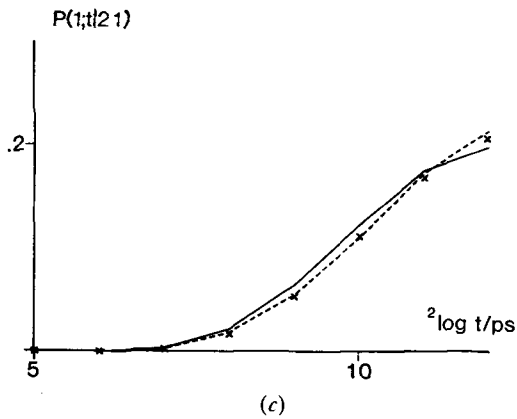
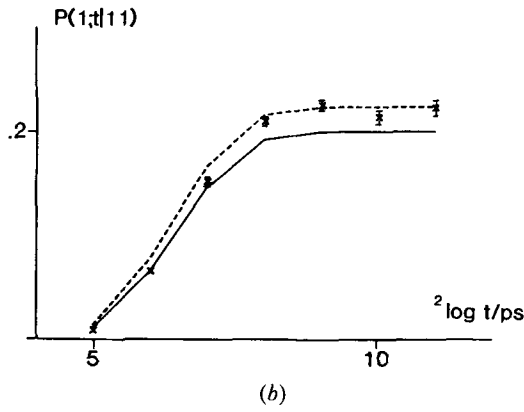
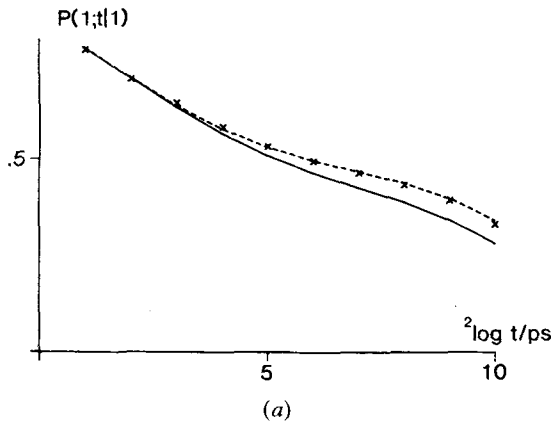


Figure 5. The transverse propagator $P(1; t | k_0)$ for monovalent ions as a function of time for three different initial positions k_0 . Symbols as in figure 3. The bars show one standard deviation for SD.

moved a short distance compared to its correlation length, which results in minor effects of dynamic correlations. However, even the propagator $P(21; t|1)$ reveals no significant relaxation effect. (This point is further discussed in § 5.3.)

Figures 6 and 7 illustrate the transverse self-diffusion of divalent counterions. As expected, static correlations are more important than for monovalent ions.

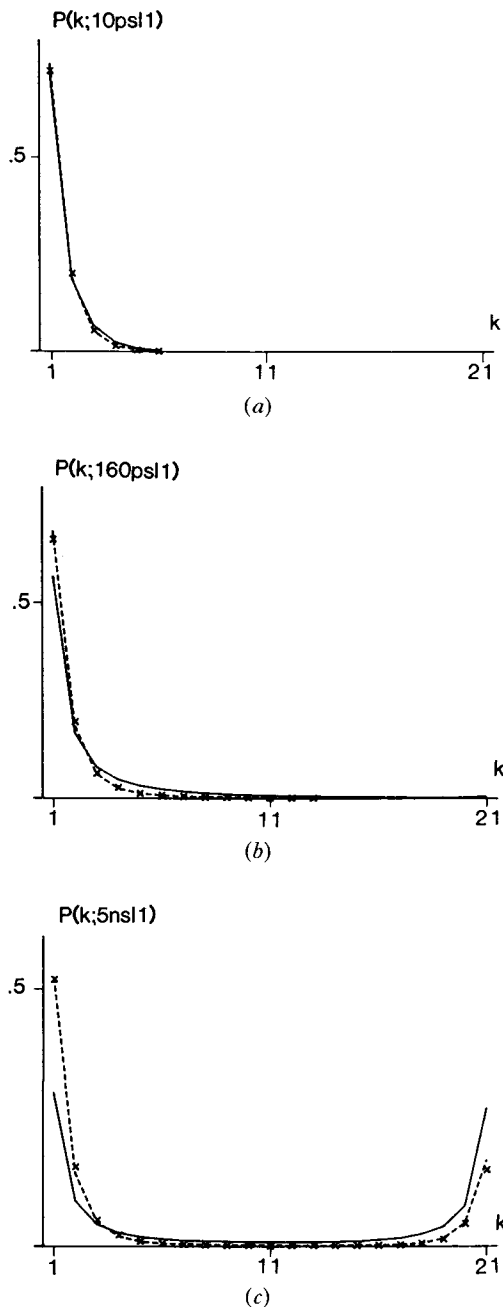


Figure 6. The transverse propagator $P(k; t|1)$ for divalent counterions as a function of k at (a) $t = 10$ ps, (b) $t = 160$ ps, and (c) $t = 5000$ ps. Symbols as in figure 3.

However, dynamic correlations are still negligible; the SD and IRA propagators are virtually identical.

An alternative to the plots in figures 5 (a) and 7 is shown in figure 8, where we have plotted the quantity $[1 - P(1; t|1)]/[1 - P_{eq}(1)]$ as function of time. This

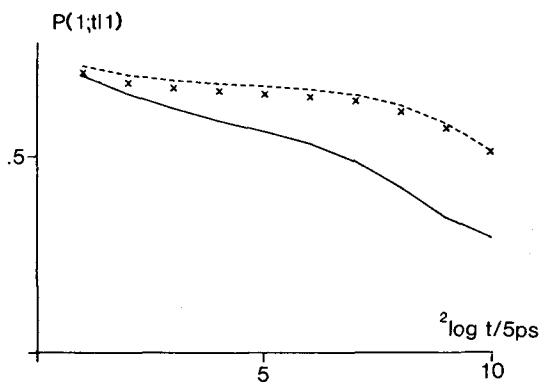


Figure 7. The time dependence of the transverse propagator $P(1; t|1)$ for divalent counterions. Symbols as in figure 3.

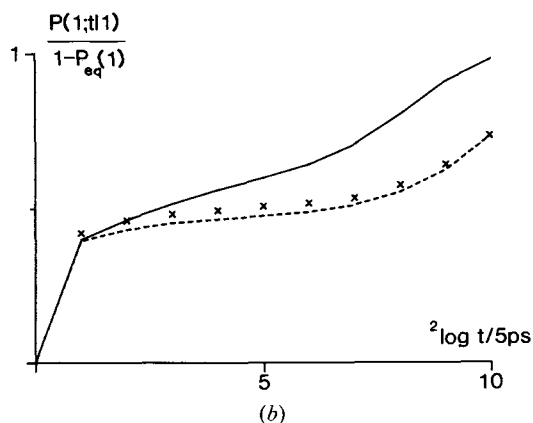
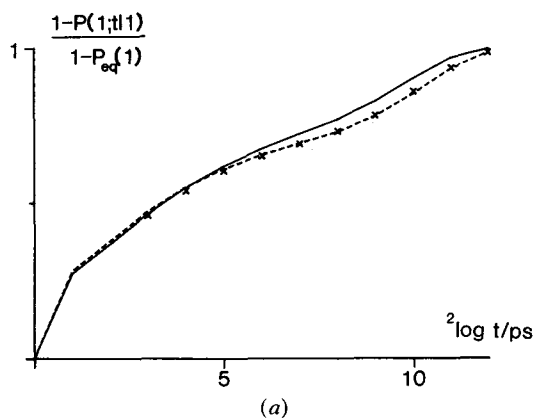


Figure 8. Transverse counterion diffusion as illustrated by the time dependence of $[1 - P(1; t|1)]/[1 - P_{eq}(1)]$ for (a) monovalent and (b) divalent ions. Symbols as in figure 3.

quantity is zero initially and evolves towards unity. At very short times, where $P(1, t|1)$ is virtually unaffected by electrostatic interactions, the SD and IRA curves exceed the SPB curve in figure 8. This is simply due to the larger value of $1 - P_{\text{eq}}(1)$ in the MFA. However, at longer times there is a cross-over and the SD and IRA curves evolve more slowly than the SPB curve, due to the deeper electrostatic potential well in the presence of static correlations.

5.3. Absorption statistics

In some applications one is primarily interested in the statistics of counterion diffusion from one spatial region to another rather than in the, hitherto discussed, decay of an initial delta-function towards the equilibrium counterion distribution. The former process may be studied theoretically by introducing an absorbing boundary condition at some point where the tagged counterion loses its label. For the transverse counterion diffusion in our model system, for example, we can define the survival probability, $Q(t|z_0, z_A)$, that a counterion, initially located at z_0 , has not yet reached (and become absorbed at) z_A at time t . Choosing the left wall (at $z = -b$) as reflecting and the absorbing boundary at $-b < z_A < b$, we can express $Q(t|z_0, z_A)$ as an integral over the transverse self-propagator, $f_s(z; t|z_0)$, subject to the corresponding boundary conditions

$$Q(t|z_0, z_A) = \int_{-b}^{z_A} dz f_s(z; t|z_0). \quad (33)$$

The mean first passage time (MFPT), $\tau(z_A|z_0)$, is the average time taken for a counterion, initially located at z_0 , to reach z_A for the first time. This quantity is obtained by a further integration as

$$\tau(z_A|z_0) = \int_0^\infty dt Q(t|z_0, z_A). \quad (34)$$

The discretized versions of the absorption probability and the MFPT can be obtained directly from a simulation (SD). In the IRA, when the transverse propagator obeys equation (17), the propagator and the absorption probability can be calculated numerically as described in Appendix D. The MFPT, however, can be calculated without the need to solve equation (17). By combining equations (17), (33), (34) and the boundary conditions and then performing the integrations in equations (33) and (34) in a formal way, one obtains the simple formula [26, 27]

$$\tau(z_A|z_0) = \frac{1}{D_0} \int_{z_0}^{z_A} dz \exp[\beta w_{\text{eq}}(z)] \int_{-b}^z dz' \exp[-\beta w_{\text{eq}}(z')]. \quad (35)$$

Using this result and the simulated (exact) potential of mean force, $w_{\text{eq}}(z)$, we calculated the IRA MFPT by summation over 0.1 \AA z -intervals. The SPB absorption probability and MFPT, finally, were obtained from the general analytical results of [20].

Figure 9 shows the transverse MFPT $\tau(z|-b)$ as a function of $-b < z < 0$ for monovalent and divalent counterions. The initial position is within 0.5 \AA of the left wall ($z = -b$). (In contrast to the other data presented in this paper, figure 9 refers to a system with $b = 13 \text{ \AA}$.) The close agreement between the SD and IRA

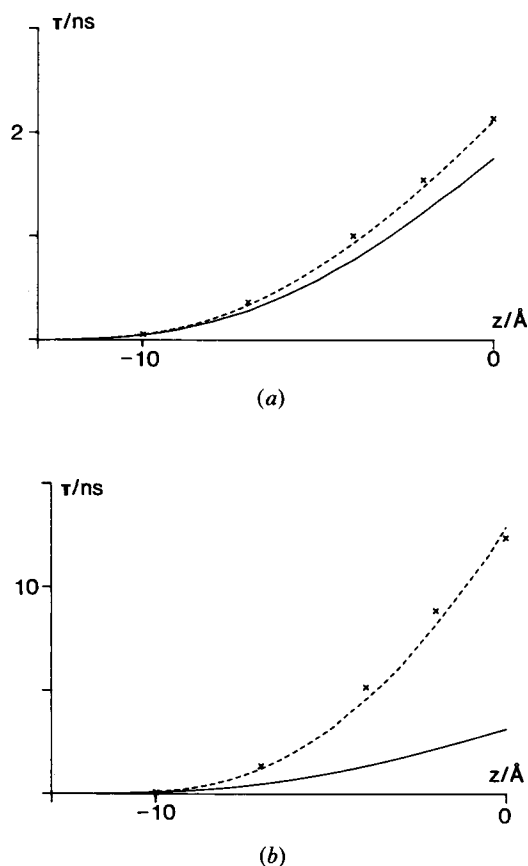


Figure 9. The MFPT $\tau(z|z_0)$ with $-b < z_0 < -b + 0.5 \text{\AA}$ for (a) monovalent and (b) divalent counterions. Symbols as in figure 3. System parameters as elsewhere, except $b = 13 \text{\AA}$.

results implies that dynamic correlations are unimportant for this MFPT. Static correlations are of minor importance for monovalent ions, for which the SPB result deviates by less than 20 percent. For divalent counterions, however, the reduced well depth in the PB potential causes the SPB approximation to $\tau(0|-b)$ to fall short by a factor of 4.

Figure 10 shows the temporal decay of the survival probability $Q(t|z_0, z_A)$, and of its logarithm, for monovalent counterions. The initial position is within 0.5\AA of the left wall and the absorbing boundary is at the midplane ($z_A = 0$). One sees again that there is virtually no effect of dynamic correlations on the counterion diffusion out of the potential well. The decay of the survival probability is seen to be exponential, except during an initial phase of ca. 200 ps. This fact may be exploited in simulations of the MFPT. Rather than extending the simulation to times that are long compared to the MFPT (which may mean up to 10^{-7} s for divalent ions), one can terminate the simulation as soon as the exponential decay in figure 10 is established and then evaluate the remainder of the integral in equation (34) analytically. This procedure may reduce the computer requirements by more than an order of magnitude.

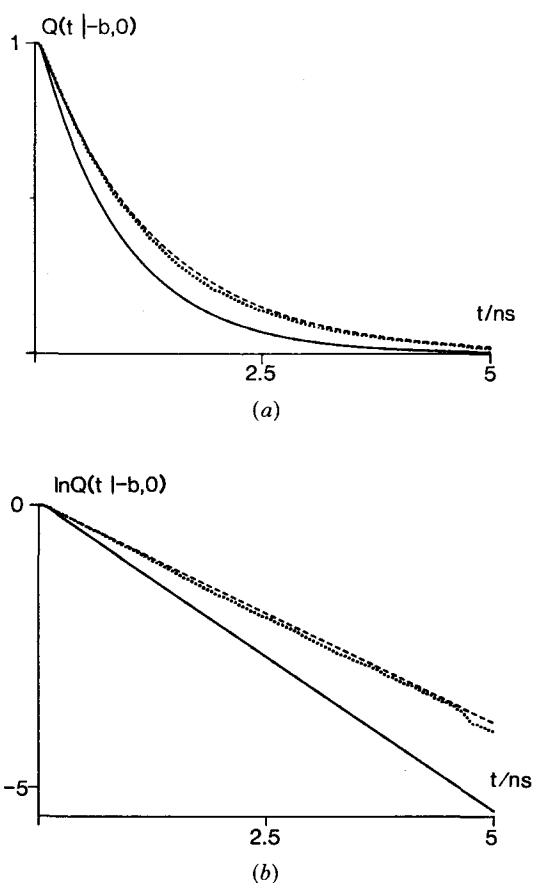


Figure 10. Time dependence of (a) the survival probability $Q(t|z_0, z_A)$ and (b) its logarithm for monovalent counterions. $z_A = 0$ and $-b < z_0 < -b + 0.5 \text{ \AA}$ with $b = 10.5 \text{ \AA}$. Symbols: SD (\cdots), IRA ($----$), SPB ($—$).

The insignificant effect of dynamic correlations on the *transverse* counterion diffusion, as evidenced by figures 9 and 10, may be contrasted with the 15 percent reduction of the effective *lateral* diffusion coefficient (figure 2). This difference can be understood as follows. The MFPT $\tau(0|-b)$ measures the time required for a counterion to escape from a well depth of several kT in the equilibrium potential of mean force. This process may be decomposed into two stages: a transient initial phase, when the position of the tagged ion becomes essentially equilibrated, followed by a quasi-steady-state phase, during which the tagged particle density slowly leaks out of the system at the absorbing boundary without significantly disturbing the equilibrium distribution. This quasi-steady-state phase, which corresponds to the exponential region in figure 10, makes the overwhelming contribution to $\tau(0|-b)$. As a consequence $\tau(0|-b)$ becomes essentially independent of dynamic correlations, which only affect the transient initial phase.

The MFPT $\tau(-b|0)$ for diffusion *into* the potential well, on the other hand, should show some effects of dynamic correlations. While we have not calculated

MFPTs, $\tau(z|b)$, from simulations compared to MFPTs obtained from equation (34) with $Q(t|-b, -z_0)$ from IRA. The quotient τ_{SD}/τ_{IRA} reflects the effect of dynamic correlations.

$z_0(\text{\AA})$	$\tau_{SD}(\text{ps})$	$\tau_{IRA}(\text{ps})$	τ_{SD}/τ_{IRA}
8	37.6	32.3	1.16
6	169	158	1.07
4	438	426	1.03
2	837	829	1.01
0	1299	1334	0.97

this MFPT, a related trend can be seen in figures 4(b) and 5(b) where the SD propagator evolves more slowly than the IRA propagator. Relaxation effects should also be apparent in $\tau(z|-b)$ for z in the neighbourhood of the charged wall; the contribution from the transient initial phase is then not negligible. Such a behaviour is illustrated by the ratio of the SD and IRA MFPT's in the table.

6. CONCLUSIONS

In this work we have investigated the statistical-mechanical basis and the numerical accuracy of the Smoluchowski–Poisson–Boltzmann approximation for describing ion diffusion in nonuniform electrolytes. Our main conclusions are as follows.

The many-particle generalized Smoluchowski equation may be formally reduced to a diffusion equation for the one-particle self-propagator. This equation contains a time-dependent generalization of the equilibrium potential of mean force. Two approximations, expressible in terms of well-defined one- and two-particle distribution functions, are needed to derive the SPB equation. These are an Instantaneous Relaxation Approximation (IRA), corresponding to the neglect of dynamic correlations (or the relaxation effect), and a Mean Field Approximation (MFA), corresponding to the neglect of static correlations.

In the investigated model system, the effective diffusion coefficient for lateral displacements of monovalent counterions is reduced by up to 15 per cent due to a relaxation effect (dynamic correlations). This reduction depends rather weakly on the distance from the charged walls.

The transverse diffusion of mono- and divalent counterions out of the well in the equilibrium potential of mean force is virtually unaffected by dynamic correlations but is sensitive to the well depth. For this mode of diffusion the IRA is thus an excellent approximation; as long as an accurate equilibrium potential of mean force is used, the dynamical behaviour is faithfully described in the IRA. The MFA (i.e. the Poisson–Boltzmann approximation) should be useful for monovalent ions, but can lead to substantial error in the dynamical description of polyvalent ions.

This work was supported by grants from the Swedish Natural Science Research Council. One of us (Bo Jönsson) also wants to acknowledge a Visiting Fellowship at the Australian National University, Canberra.

APPENDIX A

Time dependent distribution functions

We consider a collection of N identical classical solute particles without internal degrees of freedom. The system is in thermal equilibrium at a temperature T . The solvent-averaged hamiltonian of the system is

$$H(\mathbf{r}^N, \mathbf{p}^N) = \sum_{i=1}^N \frac{p_i^2}{2m} + V(\mathbf{r}^N), \quad (\text{A } 1)$$

where \mathbf{r}^N denotes the $3N$ particle coordinates $\mathbf{r}_1, \mathbf{r}_2, \dots, \mathbf{r}_N$ and \mathbf{p}^N denotes the $3N$ particle momenta $\mathbf{p}_1, \mathbf{p}_2, \dots, \mathbf{p}_N$. The potential energy of the system in the configuration \mathbf{r}^N is

$$V(\mathbf{r}^N) = \sum_{i=1}^N u_1(\mathbf{r}_i) + \frac{1}{2} \sum_{i=1}^N \sum'_{j=1}^N u_2(\mathbf{r}_i, \mathbf{r}_j), \quad (\text{A } 2)$$

where the prime signifies exclusion of the $j = i$ term. The singlet potentials $u_1(\mathbf{r}_i)$, which include the effects of confining boundaries, produce a spatially nonuniform average particle density at equilibrium.

Let $F(\mathbf{r}^N; t | \mathbf{r}_0^N)$ be the specific N -particle probability density in the canonical ensemble. Then $F(\mathbf{r}^N; t | \mathbf{r}_0^N) d\mathbf{r}^N$ is the probability of finding, at time t , the N distinct particles (labelled $1, 2, \dots, N$) to within $d\mathbf{r}^N$ of the configuration \mathbf{r}^N , given that they were in the configuration \mathbf{r}_0^N at $t = 0$. It follows that

$$\int d\mathbf{r}^N F(\mathbf{r}^N; t | \mathbf{r}_0^N) = 1. \quad (\text{A } 3)$$

Furthermore,

$$F(\mathbf{r}^N; 0 | \mathbf{r}_0^N) = \prod_{i=1}^N \delta(\mathbf{r}_i - \mathbf{r}_{0i}), \quad (\text{A } 4)$$

and

$$F(\mathbf{r}^N; \infty | \mathbf{r}_0^N) = F_{\text{eq}}(\mathbf{r}^N) = \frac{\exp[-\beta V(\mathbf{r}^N)]}{\int d\mathbf{r}^N \exp[-\beta V(\mathbf{r}^N)]}, \quad (\text{A } 5)$$

where $\beta \equiv (k_B T)^{-1}$.

The reduced specific n -particle probability densities are defined through

$$F(\mathbf{r}^n; t | \mathbf{r}_0^N) \equiv \int d\mathbf{r}^{N-n} F(\mathbf{r}^N; t | \mathbf{r}_0^N); \quad n \leq N. \quad (\text{A } 6)$$

$F(\mathbf{r}^n; t | \mathbf{r}_0^N) d\mathbf{r}^n$ is the probability of finding, at time t , n distinct particles (labelled $1, 2, \dots, n$) to within $d\mathbf{r}^n$ of the configuration \mathbf{r}^n , irrespective of the present configuration of the remaining $N - n$ particles, but conditional on the specified initial configuration of all the N particles. From equations (A 3)–(A 6), it follows that

$$\int d\mathbf{r}^n F(\mathbf{r}^n; t | \mathbf{r}_0^N) = 1, \quad (\text{A } 7)$$

$$F(\mathbf{r}^n; 0 | \mathbf{r}_0^N) = \prod_{i=1}^n \delta(\mathbf{r}_i - \mathbf{r}_{0i}), \quad (\text{A } 8)$$

$$F(\mathbf{r}^n; \infty | \mathbf{r}_0^N) = F_{\text{eq}}(\mathbf{r}^n) = \frac{\int d\mathbf{r}^{N-n} \exp[-\beta V(\mathbf{r}^N)]}{\int d\mathbf{r}^N \exp[-\beta V(\mathbf{r}^N)]}. \quad (\text{A } 9)$$

The equilibrium specific n -particle correlation functions $G_{\text{eq}}(\mathbf{r}^n)$ are defined through

$$F_{\text{eq}}(\mathbf{r}^n) \equiv G_{\text{eq}}(\mathbf{r}^n) \prod_{i=1}^n F_{\text{eq}}(\mathbf{r}_i); \quad n \leq N \quad (\text{A } 10)$$

$F_{\text{eq}}(\mathbf{r}_i) d\mathbf{r}_i$ is the probability of finding, at equilibrium, the i th particle to within $d\mathbf{r}_i$ of \mathbf{r}_i and $G_{\text{eq}}(\mathbf{r}^n)F_{\text{eq}}(\mathbf{r}_i) d\mathbf{r}_i$ is the conditional probability of finding, at equilibrium, the i th particle to within $d\mathbf{r}_i$ of \mathbf{r}_i , given that the other $n - 1$ particles are in the configuration \mathbf{r}^{n-1} (and irrespective of the configuration of the remaining $N - n$ particles). Clearly, $G_{\text{eq}}(\mathbf{r}_i) \equiv 1$.

We consider now a two-component system consisting of one tagged particle and $N - 1$ untagged, but otherwise identical, particles. For this system, we have the following relation between the specific (F) and generic (f) probability densities

$$f(\mathbf{r}^{n*}, \mathbf{r}^n; t | \mathbf{r}_0^*, \mathbf{r}_0^{N-1}) = \frac{(N - 1)!}{(N - 1 - n)!} F(\mathbf{r}^{n*}, \mathbf{r}^n; t | \mathbf{r}_0^*, \mathbf{r}_0^{N-1}), \quad (\text{A } 11)$$

where \mathbf{r}^n and \mathbf{r}_0^{N-1} refer to generic configurations on the left-hand side and to specific configurations on the right-hand side. Here, and in the following, $n^* = 0$ or 1 and $0 \leq n \leq N - 1$. In analogy with equation (A 10), the equilibrium generic ($n^* + n$)-particle correlation functions $g_{\text{eq}}(\mathbf{r}^{n*}, \mathbf{r}^n)$ are defined through

$$f_{\text{eq}}(\mathbf{r}^{n*}, \mathbf{r}^n) \equiv g_{\text{eq}}(\mathbf{r}^{n*}, \mathbf{r}^n) \prod_{i=1}^{n+n^*} f_{\text{eq}}(\mathbf{r}_i). \quad (\text{A } 12)$$

Combination of equations (A 10)–(A 12) yields a relation between the specific (G) and generic (g) correlation functions

$$g_{\text{eq}}(\mathbf{r}^{n*}, \mathbf{r}^n) = \frac{(N - 1)!}{(N - 1)^n (N - 1 - n)!} G_{\text{eq}}(\mathbf{r}^{n*}, \mathbf{r}^n). \quad (\text{A } 13)$$

Noting that

$$f_{\text{eq}}(\mathbf{r}^{n*}, \mathbf{r}^n) = \frac{1}{(N - 1 - n)!} \int d\mathbf{r}^{N-1-n} f_{\text{eq}}(\mathbf{r}^{n*}, \mathbf{r}^{N-1}) \quad (\text{A } 14)$$

and integrating equation (A 12) with $n = N - 1$, we obtain

$$\frac{1}{(N - 1 - n)!} \int d\mathbf{r}^{N-1-n} g_{\text{eq}}(\mathbf{r}^{n*}, \mathbf{r}^{N-1}) \prod_{i=n+1}^{N-1} f_{\text{eq}}(\mathbf{r}_i) = g_{\text{eq}}(\mathbf{r}^{n*}, \mathbf{r}^n). \quad (\text{A } 15)$$

This relation will be used in the following.

We now define reduced generic $(n^* + n)$ -particle probability densities with the initial configuration of the $N - 1$ untagged particles averaged over the specific conditional equilibrium probability density with the tagged particle fixed at its initial position \mathbf{r}_0^* ;

$$\begin{aligned} f(\mathbf{r}^{n^*}, \mathbf{r}^n; t | \mathbf{r}_0^*) &\equiv \frac{(N-1)!}{(N-1-n)!} \int d\mathbf{r}_0^{N-1} \left[G_{\text{eq}}(\mathbf{r}_0^*, \mathbf{r}_0^{N-1}) \prod_{i=1}^{N-1} F_{\text{eq}}(\mathbf{r}_{0i}) \right] \\ &\quad \times F(\mathbf{r}^{n^*}, \mathbf{r}^n; t | \mathbf{r}_0^*, \mathbf{r}_0^{N-1}) \\ &= \frac{1}{(N-1-n)!} \int d\mathbf{r}_0^{N-1} \left[g_{\text{eq}}(\mathbf{r}_0^*, \mathbf{r}_0^{N-1}) \prod_{i=1}^{N-1} f_{\text{eq}}(\mathbf{r}_{0i}) \right] \\ &\quad \times F(\mathbf{r}^{n^*}, \mathbf{r}^n; t | \mathbf{r}_0^*, \mathbf{r}_0^{N-1}). \end{aligned} \quad (\text{A } 16)$$

The initial condition follows from equations (A 8), (A 15) and (A 16)

$$f(\mathbf{r}^{n^*}, \mathbf{r}^n; 0 | \mathbf{r}_0^*) = \delta(\mathbf{r}^{n^*} - \mathbf{r}_0^{n^*}) g_{\text{eq}}(\mathbf{r}_0^*, \mathbf{r}^n) \prod_{i=1}^n f_{\text{eq}}(\mathbf{r}_i), \quad (\text{A } 17)$$

with the convention $\delta(\mathbf{r}^{n^*} - \mathbf{r}_0^{n^*}) \equiv 1$ for $n^* = 0$. Similarly, from equations (A 9), (A 11), (A 12), (A 15) and (A 16) we get

$$f(\mathbf{r}^{n^*}, \mathbf{r}^n; \infty | \mathbf{r}_0^*) = g_{\text{eq}}(\mathbf{r}^{n^*}, \mathbf{r}^n) \prod_{i=1}^{n+n^*} f_{\text{eq}}(\mathbf{r}_i). \quad (\text{A } 18)$$

The normalization condition follows from equations (A 7), (A 11), (A 15) and (A 16)

$$\int d\mathbf{r}^{n+n^*} f(\mathbf{r}^{n^*}, \mathbf{r}^n; t | \mathbf{r}_0^*) = \frac{(N-1)!}{(N-1-n)!}. \quad (\text{A } 19)$$

The self-propagator $f_s(\mathbf{r}^*; t | \mathbf{r}_0^*)$ is obtained by setting $n^* = 1$ and $n = 0$. According to equations (A 17)–(A 19), it obeys the following relations

$$f_s(\mathbf{r}^*; 0 | \mathbf{r}_0^*) = \delta(\mathbf{r}^* - \mathbf{r}_0^*), \quad (\text{A } 20)$$

$$f_s(\mathbf{r}^*; \infty | \mathbf{r}_0^*) = f_{\text{eq}}(\mathbf{r}^*), \quad (\text{A } 21)$$

$$\int d\mathbf{r}^* f_s(\mathbf{r}^*; t | \mathbf{r}_0^*) = 1. \quad (\text{A } 22)$$

Similarly, we obtain for the distinct propagator $f_d(\mathbf{r}; t | \mathbf{r}_0^*)$, corresponding to $n^* = 0$ and $n = 1$,

$$f_d(\mathbf{r}; 0 | \mathbf{r}_0^*) = g_{\text{eq}}(\mathbf{r}_0^*, \mathbf{r}) f_{\text{eq}}(\mathbf{r}), \quad (\text{A } 23)$$

$$f_d(\mathbf{r}; \infty | \mathbf{r}_0^*) = f_{\text{eq}}(\mathbf{r}), \quad (\text{A } 24)$$

$$\int d\mathbf{r} f_d(\mathbf{r}; t | \mathbf{r}_0^*) = N - 1. \quad (\text{A } 25)$$

The self- and distinct propagators just defined constitute the generalizations of van Hove's self- and distinct space-time correlation functions to nonuniform systems.

The pair propagator $f(\mathbf{r}^*, \mathbf{r}; t | \mathbf{r}_0^*)$ is obtained by setting $n^* = n = 1$. The quantity $f(\mathbf{r}^*, \mathbf{r}; t | \mathbf{r}_0^*) d\mathbf{r}^* d\mathbf{r}$ is the probability of finding, at time t , the tagged particle to within $d\mathbf{r}^*$ of \mathbf{r}^* and any one of the $N - 1$ untagged particles to within $d\mathbf{r}$ of \mathbf{r} , irrespective of the configuration of the remaining $N - 2$ untagged particles, and with the initial configuration of the $N - 1$ untagged particles averaged over the conditional equilibrium probability density with the tagged particle fixed at \mathbf{r}_0^* . From equations (A 17)–(A 19) it follows that

$$f(\mathbf{r}^*, \mathbf{r}; 0 | \mathbf{r}_0^*) = \delta(\mathbf{r}^* - \mathbf{r}_0^*) g_{\text{eq}}(\mathbf{r}_0^*, \mathbf{r}) f_{\text{eq}}(\mathbf{r}), \tag{A 26}$$

$$f(\mathbf{r}^*, \mathbf{r}; \infty | \mathbf{r}_0^*) = f_{\text{eq}}(\mathbf{r}^*) g_{\text{eq}}(\mathbf{r}^*, \mathbf{r}) f_{\text{eq}}(\mathbf{r}), \tag{A 27}$$

$$\int d\mathbf{r}^* \int d\mathbf{r} f(\mathbf{r}^*, \mathbf{r}; t | \mathbf{r}_0^*) = N - 1. \tag{A 28}$$

Finally, we define time dependent (or ‘nonequilibrium’) generic $(n^* + n)$ -particle correlation functions $g(\mathbf{r}^{n^*}, \mathbf{r}^n; t | \mathbf{r}_0^*)$ through

$$f(\mathbf{r}^{n^*}, \mathbf{r}^n; t | \mathbf{r}_0^*) \equiv g(\mathbf{r}^{n^*}, \mathbf{r}^n; t | \mathbf{r}_0^*) \prod_{i=1}^{n+n^*} f(\mathbf{r}_i; t | \mathbf{r}_0^*). \tag{A 29}$$

This is the time dependent generalization of equation (A 13). Clearly, $g \equiv 1$ for $n + n^* \leq 1$. From equations (A 17), (A 18) and (A 29) it follows that

$$g(\mathbf{r}^{n^*}, \mathbf{r}^n; 0 | \mathbf{r}_0^*) = \frac{g_{\text{eq}}(\mathbf{r}_0^*, \mathbf{r}^n)}{\prod_{i=1}^n g_{\text{eq}}(\mathbf{r}_0^*, \mathbf{r}_i)}, \tag{A 30}$$

$$g(\mathbf{r}^{n^*}, \mathbf{r}^n; \infty | \mathbf{r}_0^*) = g_{\text{eq}}(\mathbf{r}^{n^*}, \mathbf{r}^n). \tag{A 31}$$

From equations (A 29)–(A 31), we obtain for the time dependent pair correlation function ($n^* = n = 1$)

$$f(\mathbf{r}^*, \mathbf{r}; t | \mathbf{r}_0^*) \equiv f_s(\mathbf{r}^*; t | \mathbf{r}_0^*) g(\mathbf{r}^*, \mathbf{r}; t | \mathbf{r}_0^*) f_d(\mathbf{r}; t | \mathbf{r}_0^*), \tag{A 32}$$

$$g(\mathbf{r}^*, \mathbf{r}; 0 | \mathbf{r}_0^*) = 1, \tag{A 33}$$

$$g(\mathbf{r}^*, \mathbf{r}; \infty | \mathbf{r}_0^*) = g_{\text{eq}}(\mathbf{r}^*, \mathbf{r}). \tag{A 34}$$

APPENDIX B

Derivation of generalized Smoluchowski equations

The N -particle generalized Smoluchowski equation, equation (2), may also be expressed as a continuity equation

$$\frac{\partial}{\partial t} F(\mathbf{r}^N; t | \mathbf{r}_0^N) + \sum_{i=1}^N \nabla_i \cdot \mathbf{J}_i(\mathbf{r}^N; t | \mathbf{r}_0^N) = 0, \tag{B 1}$$

with the fluxes

$$\mathbf{J}_i(\mathbf{r}^N; t | \mathbf{r}_0^N) \equiv -D_0 \left\{ \nabla_i F(\mathbf{r}^N; t | \mathbf{r}_0^N) + \beta \nabla_i \left[u_1(\mathbf{r}_i) + \sum_{j=1}^N u_2(\mathbf{r}_i, \mathbf{r}_j) \right] F(\mathbf{r}^N; t | \mathbf{r}_0^N) \right\}. \tag{B 2}$$

Since the system is closed, the boundary conditions are

$$\hat{\mathbf{n}}(\mathbf{r}_i) \cdot \mathbf{J}_i(\mathbf{r}^N; t | \mathbf{r}_0^N) \Big|_{\mathbf{r}_i \text{ on } S} = 0; \quad i = 1, 2, \dots, N, \tag{B 3}$$

where $\hat{\mathbf{n}}(\mathbf{r}_i)$ is the outward-pointing normal unit vector at a point \mathbf{r}_i on the bounding surface S .

We shall now derive the generalized Smoluchowski equation obeyed by the self-propagator $f_s(\mathbf{r}^*; t | \mathbf{r}_0^*)$ defined in Appendix A. Consider the set of operators

$$\hat{P}_n \equiv \frac{1}{(N-1-n)!} \int d\mathbf{r}_0^{N-1} g_{\text{eq}}(\mathbf{r}_0^*, \mathbf{r}_0^{N-1}) \prod_{i=1}^{N-1} f_{\text{eq}}(\mathbf{r}_{0i}) \int d\mathbf{r}^{N-1-n}; \tag{B 4}$$

$n = 0, 1, \dots, N-1,$

which, according to equations (A 6) and (A 16), effect the transformations

$$\hat{P}_n F(\mathbf{r}^N; t | \mathbf{r}_0^N) = f(\mathbf{r}^*, \mathbf{r}^n; t | \mathbf{r}_0^*). \tag{B 5}$$

From equation (B 4), we see that the following recursive relation is obeyed

$$\hat{P}_n = (N-1-n)^{-1} \hat{P}_{n+1} \int d\mathbf{r}. \tag{B 6}$$

Operating on equation (B 1) with \hat{P}_0 and using equation (B 5), we get

$$\frac{\partial}{\partial t} f_s(\mathbf{r}^*; t | \mathbf{r}_0^*) + \nabla^* \cdot \hat{P}_0 \mathbf{J}^*(\mathbf{r}^N; t | \mathbf{r}_0^N) + \sum_{i=1}^{N-1} \hat{P}_0 \nabla_i \cdot \mathbf{J}_i(\mathbf{r}^N; t | \mathbf{r}_0^N) = 0. \tag{B 7}$$

Using, in turn, equation (B 6), the divergence theorem and the boundary conditions, equation (B 3), we can get rid of the sum in equation (B 7) as follows

$$\begin{aligned} \sum_{i=1}^{N-1} \hat{P}_0 \nabla_i \cdot \mathbf{J}_i(\mathbf{r}^N; t | \mathbf{r}_0^N) &= (N-1)^{-1} \sum_{i=1}^{N-1} \hat{P}_1 \int_V d\mathbf{r}_i \nabla_i \cdot \mathbf{J}_i(\mathbf{r}^N; t | \mathbf{r}_0^N) \\ &= (N-1)^{-1} \sum_{i=1}^{N-1} \hat{P}_1 \int_S d\sigma_i \hat{\mathbf{n}}(\mathbf{r}_i) \cdot \mathbf{J}_i(\mathbf{r}^N; t | \mathbf{r}_0^N) \\ &= 0. \end{aligned} \tag{B 8}$$

Furthermore, from equation (B 2) we have

$$\begin{aligned} \hat{P}_0 \mathbf{J}^*(\mathbf{r}^N; t | \mathbf{r}_0^N) &= -D_0 \left\{ \nabla^* f_s(\mathbf{r}^*; t | \mathbf{r}_0^*) + \beta [\nabla^* u_1(\mathbf{r}^*)] f_s(\mathbf{r}^*; t | \mathbf{r}_0^*) \right. \\ &\quad \left. + \beta \sum_{i=1}^{N-1} \hat{P}_0 [\nabla^* u_2(\mathbf{r}^*, \mathbf{r}_i)] F(\mathbf{r}^N; t | \mathbf{r}_0^N) \right\}. \end{aligned} \tag{B 9}$$

Using equations (B 5) and (B 6), the last term of equation (B 9) may be transformed as follows

$$\begin{aligned} \sum_{i=1}^{N-1} \hat{P}_0 [\nabla^* u_2(\mathbf{r}^*, \mathbf{r}_i)] F(\mathbf{r}^N; t | \mathbf{r}_0^N) &= (N-1)^{-1} \sum_{i=1}^{N-1} \int d\mathbf{r}_i [\nabla^* u_2(\mathbf{r}^*, \mathbf{r}_i)] \hat{P}_1 F(\mathbf{r}^N; t | \mathbf{r}_0^N) \\ &= \int d\mathbf{r} [\nabla^* u_2(\mathbf{r}^*, \mathbf{r})] f(\mathbf{r}^*, \mathbf{r}; t | \mathbf{r}_0^*). \end{aligned} \tag{B 10}$$

Combining equations (B7)–(B10) and using equation (A32), we arrive at the desired result

$$\begin{aligned} \frac{\partial}{\partial t} f_s(\mathbf{r}^*; t | \mathbf{r}_0^*) &= D_0 \nabla^* \cdot \left\{ \nabla^* f_s(\mathbf{r}^*; t | \mathbf{r}_0^*) + \beta [\nabla^* u_1(\mathbf{r}^*)] f_s(\mathbf{r}^*; t | \mathbf{r}_0^*) \right. \\ &\quad \left. + \beta \left[\int d\mathbf{r} [\nabla^* u_2(\mathbf{r}^*, \mathbf{r})] g(\mathbf{r}^*, \mathbf{r}; t | \mathbf{r}_0^*) f_d(\mathbf{r}; t | \mathbf{r}_0^*) \right] f_s(\mathbf{r}^*; t | \mathbf{r}_0^*) \right\}. \end{aligned} \quad (\text{B } 11)$$

A similar derivation leads to the generalized Smoluchowski equation for the distinct propagator. The result is

$$\begin{aligned} \frac{\partial}{\partial t} f_d(\mathbf{r}; t | \mathbf{r}_0^*) &= D_0 \nabla \cdot \left\{ \nabla f_d(\mathbf{r}; t | \mathbf{r}_0^*) + \beta [\nabla u_1(\mathbf{r})] f_d(\mathbf{r}; t | \mathbf{r}_0^*) \right. \\ &\quad + \beta \left[\int d\mathbf{r}' [\nabla u_2(\mathbf{r}', \mathbf{r})] g(\mathbf{r}', \mathbf{r}; t | \mathbf{r}_0^*) f_d(\mathbf{r}'; t | \mathbf{r}_0^*) \right] f_d(\mathbf{r}; t | \mathbf{r}_0^*) \\ &\quad \left. + \beta \left[\int d\mathbf{r}^* [\nabla u_2(\mathbf{r}^*, \mathbf{r})] g(\mathbf{r}^*, \mathbf{r}; t | \mathbf{r}_0^*) f_s(\mathbf{r}^*; t | \mathbf{r}_0^*) \right] f_d(\mathbf{r}; t | \mathbf{r}_0^*) \right\}. \end{aligned} \quad (\text{B } 12)$$

APPENDIX C

Solution of the planar Smoluchowski–Poisson–Boltzmann equation

Introducing the dimensionless variables

$$\xi \equiv \kappa z, \quad (\text{C } 1)$$

$$\tau \equiv \kappa^2 D_0 t \quad (\text{C } 2)$$

and the dimensionless propagator

$$\tilde{f}_s(\xi; \tau | \xi_0) \equiv \kappa^{-1} f_s(\xi; t | \xi_0), \quad (\text{C } 3)$$

the SPB equation for planar geometry, equation (19), becomes

$$\frac{\partial}{\partial \tau} \tilde{f}_s(\xi; \tau | \xi_0) = \frac{\partial}{\partial \xi} \left[\left(\frac{\partial}{\partial \xi} - 2 \tan \xi \right) \tilde{f}_s(\xi; \tau | \xi_0) \right]. \quad (\text{C } 4)$$

The walls at $\xi = \pm \kappa b$ are impenetrable, so the boundary conditions are

$$\tilde{f}'_s(-\kappa b; \tau | \xi_0) + 2 \tan(\kappa b) \tilde{f}_s(-\kappa b; \tau | \xi_0) = 0, \quad (\text{C } 5 a)$$

$$\tilde{f}'_s(\kappa b; \tau | \xi_0) - 2 \tan(\kappa b) \tilde{f}_s(\kappa b; \tau | \xi_0) = 0, \quad (\text{C } 5 b)$$

where prime denotes differentiation with respect to ξ . Furthermore, we have the initial condition

$$\tilde{f}_s(\xi; 0 | \xi_0) = \delta(\xi - \xi_0). \quad (\text{C } 6)$$

We attempt a solution of the form

$$\tilde{f}_s(\xi; \tau | \xi_0) = \Xi(\xi)Y(\tau). \quad (\text{C } 7)$$

Substitution into equation (C 4) yields

$$\frac{Y'(\tau)}{Y(\tau)} = \frac{\Xi''(\xi)}{\Xi(\xi)} - 2 \tan \xi \frac{\Xi'(\xi)}{\Xi(\xi)} - 2 \sec^2 \xi = -(\lambda^2 - 1), \quad (\text{C } 8)$$

where we have denoted the separation constant by $-(\lambda^2 - 1)$. The time dependent part of the solution is obtained immediately from equation (C 8) as

$$Y(\tau) = \exp [-(\lambda^2 - 1)\tau]. \quad (\text{C } 9)$$

The spatial part is the solution to the second-order ordinary differential equation

$$\Xi''(\xi) - 2 \tan \xi \Xi'(\xi) + [\lambda^2 - 1 - 2 \sec^2 \xi] \Xi(\xi) = 0. \quad (\text{C } 10)$$

By introducing the new dependent variable

$$y(\xi) \equiv \cos \xi \Xi(\xi) \quad (\text{C } 11)$$

we can transform equation (C 10) into normal form, lacking the first derivative,

$$y''(\xi) + [\lambda^2 - 2 \sec^2 \xi] y(\xi) = 0. \quad (\text{C } 12)$$

As can easily be verified, the general solution to equation (C 12) is

$$y(\xi) = \alpha[\tan \xi \cos(\lambda\xi) - \lambda \sin(\lambda\xi)] + \beta[\tan \xi \sin(\lambda\xi) + \lambda \cos(\lambda\xi)], \quad (\text{C } 13)$$

where α and β are constants to be determined from the initial and boundary conditions.

The boundary conditions on $y(\xi)$ follow from equations (C 5), (C 7) and (C 11)

$$y'(-\kappa b) + \tan(\kappa b)y(-\kappa b) = 0, \quad (\text{C } 14 a)$$

$$y'(\kappa b) - \tan(\kappa b)y(\kappa b) = 0. \quad (\text{C } 14 b)$$

Inserting $y(\xi)$ and $y'(\xi)$ from equation (C 13) into equation (C 14), we find

$$\alpha(1 - \lambda^2) \cos(\lambda\kappa b) - \beta(1 - \lambda^2) \sin(\lambda\kappa b) = 0, \quad (\text{C } 15 a)$$

$$\alpha(1 - \lambda^2) \cos(\lambda\kappa b) + \beta(1 - \lambda^2) \sin(\lambda\kappa b) = 0. \quad (\text{C } 15 b)$$

From equation (C 9), it is seen that the solution $\lambda^2 = 1$ corresponds to the time independent equilibrium distribution, which is given by

$$\tilde{f}_{\text{eq}}(\xi) = \frac{1}{2} \cot(\kappa b) \sec^2 \xi \quad (\text{C } 16)$$

in accordance with equation (13). The remaining non-trivial solutions of equation (C 15) are obtained by requiring the determinant of the coefficients of α and β to vanish. This leads to the eigenvalue equation

$$\sin(2\kappa b\lambda_n) = 0 \quad (\text{C } 17)$$

with the solutions

$$\lambda_n = \frac{n\pi}{2\kappa b}; \quad n = 1, 2, \dots \quad (\text{C } 18)$$

On substituting the eigenvalues, equation (C 18), back into equation (C 15), we find

$$\left. \begin{aligned} \alpha &= 0; & n \text{ even,} \\ \beta &= 0; & n \text{ odd.} \end{aligned} \right\} \tag{C 19}$$

When this result is combined with equations (C 7), (C 9), (C 11), (C 13) and (C 16), we get

$$\begin{aligned} \tilde{f}_s(\xi; \tau | \xi_0) &= \frac{1}{2} \cot \kappa b \sec^2 \xi \\ &+ \sec \xi \sum_{n=1}^{\infty} [\delta_{n, \text{ odd}} \alpha_n u_n(\xi) + (1 - \delta_{n, \text{ odd}}) \beta_n v_n(\xi)] \exp [-(\lambda_n^2 - 1)\tau], \end{aligned} \tag{C 20}$$

where $\delta_{n, \text{ odd}} = 1$ if n is odd and 0 otherwise and where

$$u_n(\xi) \equiv \tan \xi \cos (\lambda_n \xi) - \lambda_n \sin (\lambda_n \xi), \tag{C 21 a}$$

$$v_n(\xi) \equiv \tan \xi \sin (\lambda_n \xi) + \lambda_n \cos (\lambda_n \xi). \tag{C 21 b}$$

Using equation (C 18), we obtain the orthogonality relations

$$\int_{-\kappa b}^{\kappa b} d\xi u_m(\xi)u_n(\xi) = \delta_{mn} \kappa b (\lambda_n^2 - 1); \quad n \text{ odd,} \tag{C 22 a}$$

$$\int_{-\kappa b}^{\kappa b} d\xi v_m(\xi)v_n(\xi) = \delta_{mn} \kappa b (\lambda_n^2 - 1); \quad n \text{ even,} \tag{C 22 b}$$

$$\int_{-\kappa b}^{\kappa b} d\xi u_m(\xi)v_n(\xi) = 0. \tag{C 22 c}$$

The coefficients α_n and β_n in equation (C 20) are determined by the initial condition, equation (C 6), which yields

$$\frac{1}{2} \cot \kappa b \sec^2 \xi + \sec \xi \sum_{n=1}^{\infty} [\delta_{n, \text{ odd}} \alpha_n u_n(\xi) + (1 - \delta_{n, \text{ odd}}) \beta_n v_n(\xi)] = \delta(\xi - \xi_0). \tag{C 23}$$

Multiplying equation (C 23) by $\cos \xi u_m(\xi)$ (m odd) or by $\cos \xi v_m(\xi)$ (m even) and integrating over ξ using equation (C 22), we obtain

$$\alpha_n = \frac{\cos \xi_0 u_n(\xi_0)}{\kappa b (\lambda_n^2 - 1)}, \tag{C 24 a}$$

$$\beta_n = \frac{\cos \xi_0 v_n(\xi_0)}{\kappa b (\lambda_n^2 - 1)}. \tag{C 24 b}$$

Substitution into equation (C 20) then leads to the final solution

$$\begin{aligned} \tilde{f}_s(\xi; \tau | \xi_0) &= \frac{1}{2} \cot \kappa b \sec^2 \xi + \frac{1}{\kappa b} \frac{\cos \xi_0}{\cos \xi} \\ &\times \sum_{n=1}^{\infty} [\delta_{n, \text{ odd}} u_n(\xi_0)u_n(\xi) + (1 - \delta_{n, \text{ odd}})v_n(\xi_0)v_n(\xi)] \frac{\exp [-(\lambda_n^2 - 1)\tau]}{(\lambda_n^2 - 1)}. \end{aligned} \tag{C 25}$$

For the purpose of comparison with propagators obtained by way of stochastic dynamics simulations, it is desirable to discretize equation (C 25). Let the ξ -range be divided into intervals of equal width $\Delta' \equiv k\Delta$, numbered from left to right. If

$P(k; \tau | k_0)$ is the probability of finding the tagged counterion in the k th interval at τ , given that it was in the k_0 th interval initially, then

$$P(k; \tau | k_0) = \frac{\int_{-\kappa b + (k_0 - 1)\Delta'}^{-\kappa b + k_0\Delta'} d\xi_0 \tilde{f}_{\text{eq}}(\xi_0) \int_{-\kappa b + (k - 1)\Delta'}^{-\kappa b + k\Delta'} d\xi \tilde{f}_s(\xi; \tau | \xi_0)}{\int_{-\kappa b + (k_0 - 1)\Delta'}^{-\kappa b + k_0\Delta'} d\xi_0 \tilde{f}_{\text{eq}}(\xi_0)}. \quad (\text{C } 26)$$

Inserting equations (C 16) and (C 25) and performing the integrations, we obtain

$$P(k; \tau | k_0) = \frac{1}{2} \cot(\kappa b) W(k) + \frac{1}{\kappa b W(k_0)} \sum_{n=1}^{\infty} [\delta_{n, \text{odd}} U_n(k_0) U_n(k) + (1 - \delta_{n, \text{odd}}) V_n(k_0) V_n(k)] \frac{\exp[-(\lambda_n^2 - 1)\tau]}{(\lambda_n^2 - 1)}, \quad (\text{C } 27)$$

where

$$U_n(k) \equiv \sec(-\kappa b + k\Delta') \cos[\lambda_n(-\kappa b + k\Delta')] - \sec[-\kappa b + (k - 1)\Delta'] \cos[\lambda_n(-\kappa b + (k - 1)\Delta')], \quad (\text{C } 28 \text{ a})$$

$$V_n(k) \equiv \sec(-\kappa b + k\Delta') \sin[\lambda_n(-\kappa b + k\Delta')] - \sec(-\kappa b + (k - 1)\Delta') \sin[\lambda_n(-\kappa b + (k - 1)\Delta')], \quad (\text{C } 28 \text{ b})$$

$$W(k) \equiv \tan(-\kappa b + k\Delta') - \tan(-\kappa b + (k - 1)\Delta'). \quad (\text{C } 28 \text{ c})$$

APPENDIX D

The Smoluchowski difference equation

In this appendix we describe a numerical algorithm for solving a discretized version of the Smoluchowski equation for diffusion perpendicular to the plates, equation (17). This is necessary when the equilibrium mean force, $-w'_{\text{eq}}(z)$, is not known analytically, but rather specified numerically as a set of averages over finite intervals.

The diffusion space, $-b \leq z \leq b$, is discretized by introducing $N + 1$ equidistant grid points $z_k = -b + k\Delta$, $k = 0, 1, 2, \dots, N$. The space is thus divided into N intervals, each of width $\Delta = 2b/N$. Similarly, the time coordinate is discretized by introducing equidistant grid points $t_l = l\Delta t$, $l = 0, 1, 2, \dots$. The self-propagator on this lattice of grid points will be denoted by $f(k, l)$.

The spatial derivatives occurring in equation (17) are approximated by the following central finite-difference formulas

$$\left. \frac{\partial}{\partial z} f_s(z; t) \right|_{z_k, t_l} = \frac{f(k + 1, l) - f(k - 1, l)}{2\Delta}, \quad (\text{D } 1)$$

$$\left. \frac{\partial^2}{\partial z^2} f_s(z; t) \right|_{z_k, t_l} = \frac{f(k + 1, l) - 2f(k, l) + f(k - 1, l)}{\Delta^2}, \quad (\text{D } 2)$$

$$\left. \frac{\partial}{\partial z} [w'(z) f_s(z; t)] \right|_{z_k, t_l} = \frac{w'(k + 1) f(k + 1, l) - w'(k - 1) f(k - 1, l)}{2\Delta}. \quad (\text{D } 3)$$

These expressions are to be used only at the internal grid points, $k = 1, 2, \dots, N - 1$. The boundary points, $k = 0$ and $k = N$, will be treated separately. The time derivative is approximated by the forward finite-difference formula

$$\left. \frac{\partial}{\partial t} f_s(z; t) \right|_{z_k, t_l} = \frac{f(k, l + 1) - f(k, l)}{\Delta t}. \tag{D 4}$$

On substituting equations (D 1)–(D 4) into equation (17), we obtain the difference equation

$$f(k, l + 1) = \alpha[1 - \frac{1}{2}\beta\Delta zw'(k - 1)]f(k - 1, l) + [1 - 2\alpha]f(k, l) + \alpha[1 + \frac{1}{2}\beta\Delta zw'(k + 1)]f(k + 1, l); \quad k = 1, 2, \dots, N - 1, \tag{D 5}$$

where we have introduced the dimensionless parameter

$$\alpha \equiv \frac{D_0 \Delta t}{\Delta^2}. \tag{D 6}$$

In order to obtain acceptable statistics in simulation data, one usually forms averages over finite intervals. For comparative purposes, it is therefore convenient to define

$$P(k, l) \equiv \int_{z_{k-1}}^{z_k} dz f_s(z; t_l); \quad k = 1, 2, \dots, N, \tag{D 7}$$

which is the probability of finding the tagged particle in the k th z -interval at time t_l . Similarly, we define

$$W'(k) \equiv \int_{z_{k-1}}^{z_k} dz w'(z); \quad k = 1, 2, \dots, N. \tag{D 8}$$

These integrals will be approximated by

$$P(k, l) = \Delta f(k, l), \tag{D 9}$$

$$W'(k) = \Delta zw'(k). \tag{D 10}$$

Substituting equations (D 9) and (D 10) into equation (D 5), and introducing matrix notation, we have

$$\mathbf{P}(l + 1) = \mathbf{TP}(l), \tag{D 11}$$

where $\mathbf{P}(l)$ is a column matrix with elements $P_k \equiv P(k, l)$, $k = 1, 2, \dots, N$. The element $T_{kk'}$ of the $N \times N$ transition matrix \mathbf{T} gives the probability for a transition from the k' th to the k th interval to occur in a time interval Δt . A comparison of equations (D 5) and (D 11) reveals that \mathbf{T} is tridiagonal with nonzero elements

$$T_{k, k-1} = \alpha[1 - \frac{1}{2}\beta W'(k - 1)]; \quad k = 2, 3, \dots, N, \tag{D 12 a}$$

$$T_{kk} = 1 - 2\alpha; \quad k = 2, 3, \dots, N - 1, \tag{D 12 b}$$

$$T_{k, k+1} = \alpha[1 + \frac{1}{2}\beta W'(k + 1)]; \quad k = 1, 2, \dots, N - 1. \tag{D 12 c}$$

The two elements T_{11} and T_{NN} are not given by equation (D 12); they must be determined from the boundary conditions. To do this, we first note that conservation of probability requires that

$$T_{k-1,k} + T_{kk} + T_{k+1,k} = 1. \quad (\text{D } 13)$$

With both boundaries reflecting, there can be no flux of probability across either z_0 or z_N . Hence, we must have $T_{01} = 0$ and $T_{N+1,N} = 0$. From equation (D 13), it then follows that

$$T_{11} = 1 - T_{21}, \quad (\text{D } 14 a)$$

$$T_{NN} = 1 - T_{N-1,N}. \quad (\text{D } 14 b)$$

Finally, we have the initial condition

$$P_k(0) = \delta_{kk_0}. \quad (\text{D } 15)$$

The algorithm is stable for $\alpha \leq \frac{1}{2}$ and the discretization error can be made arbitrarily small (at the expense of increasing the computing time) by decreasing the grid spacings.

The case with one reflecting and one absorbing boundary can be handled in an analogous way by altering a few elements in the transition matrix. With a reflecting boundary at z_0 and an absorbing boundary at z_{N_A} , we have N_A z -intervals of width $\Delta = 2b/N$. Equation (D 12) still applies if N is replaced by N_A and if the upper limit in (D 12 c) is taken as $N_A - 2$. In addition to equation (D 14 a), we now have

$$T_{N_A-1, N_A} = 0 \quad (\text{D } 16 a)$$

$$T_{N_A N_A} = 0. \quad (\text{D } 16 b)$$

The discretized survival probability, $Q(l|k_0, N_A)$, is obtained by summation as

$$Q(l|k_0, N_A) = \sum_{k=1}^{N_A} P(k, l). \quad (\text{D } 17)$$

To compensate for the error introduced by letting, in equation (D 16), the entire N_A th interval be absorbing, we calculate the corrected quantity

$$Q_{\text{corr}}(l|k_0, N_A) = \frac{1}{2}[Q(l|k_0, N_A) + Q(l|k_0, N_A + 1)]. \quad (\text{D } 18)$$

With the grid spacing used in our calculations, the error in this procedure is negligible.

REFERENCES

- [1] GOUY, G., 1910, *J. Phys. Radium, Paris*, **9**, 457.
- [2] CHAPMAN, D. L., 1913, *Phil. Mag.*, **25**, 475.
- [3] CARNIE, S. L., and TORRIE, G. M., 1984, *Adv. chem. Phys.*, **56**, 141.
- [4] WOLYNES, P. G., 1980, *An. Rev. phys. Chem.*, **31**, 345.
- [5] KATCHALSKY, A., ALEXANDROWICZ, Z., and KEDEM, O., 1966, *Chemical Physics of Ionic Solutions*, edited by B. E. Conway and R. G. Barradas (Wiley).
- [6] VON SMOLUCHOWSKI, M., 1915, *Annln Phys.*, **48**, 1103.
- [7] LIFSON, S., and JACKSON, J. L., 1962, *J. chem. Phys.*, **36**, 2410.

- [8] JACKSON, J. L., and CORIELL, S. R., 1963, *J. chem. Phys.*, **38**, 959.
- [9] BELL, G. M., and DUNNING, A. J., 1969, *Trans. Faraday Soc.*, **65**, 500.
- [10] YOSHIDA, N., 1978, *J. chem. Phys.*, **69**, 4867.
- [11] HALLE, B., 1984, *Molec. Phys.*, **53**, 1427.
- [12] HALLE, B., WENNERSTRÖM, H., and PICULELL, L., 1984, *J. phys. Chem.*, **88**, 2482.
- [13] FALKENHAGEN, H., 1934, *Electrolytes* (Clarendon).
- [14] EBELING, W., 1965, *Annl. Phys.*, **16**, 147.
- [15] MURPHY, T. J., and AGUIRRE, J. L., 1972, *J. chem. Phys.*, **57**, 2098.
- [16] WILEMSKI, G., 1976, *J. statist. Phys.*, **14**, 153.
- [17] TITULAER, U. M., 1978, *Physica A*, **91**, 321.
- [18] VAN HOVE, L., 1954, *Phys. Rev.*, **95**, 249.
- [19] JÖNSSON, B., WENNERSTRÖM, H., and HALLE, B., 1980, *J. phys. Chem.*, **84**, 2179.
- [20] CHAN, D. Y. C., and HALLE, B., 1984, *Biophys. J.*, **46**, 387.
- [21] OHNISHI, T., IMAI, N., and OOSAWA, F., 1960, *J. phys. Soc. Japan*, **15**, 896.
- [22] ENGSTRÖM, S., and WENNERSTRÖM, H., 1978, *J. phys. Chem.*, **82**, 2711.
- [23] CARSLAW, H. S., and JAEGER, J. C., 1959, *Conduction of Heat in Solids*, 2nd edition (Oxford University Press).
- [24] ÅKESSON, T., and JÖNSSON, B., 1985, *Molec. Phys.*, **54**, 369.
- [25] CHANDRASEKHAR, S., 1943, *Rev. mod. Phys.*, **15**, 1.
- [26] PONTRJAGIN, L., ANDRONOV, A., and WITT, A., 1934, *Phys. Z. SowjUn.*, **6**, 1.
- [27] DEUTCH, J. M., 1980, *J. chem. Phys.*, **73**, 4700.
- [28] GULDBRAND, L., JÖNSSON, B., WENNERSTRÖM, H., and LINSE, P., 1984, *J. chem. Phys.*, **80**, 2221.